UCRL-JC-130870
PREPRINT

OCT for Diagnosis of Periodontal Disease

B. W. Colston, Jr.
M. J. Everett
L. B. DaSilva
L. L. Otis

This paper was prepared for submittal to the
Society of Photo-Optical Instrumentation Engineers
San Jose, CA
January 24-30, 1998

January 1998

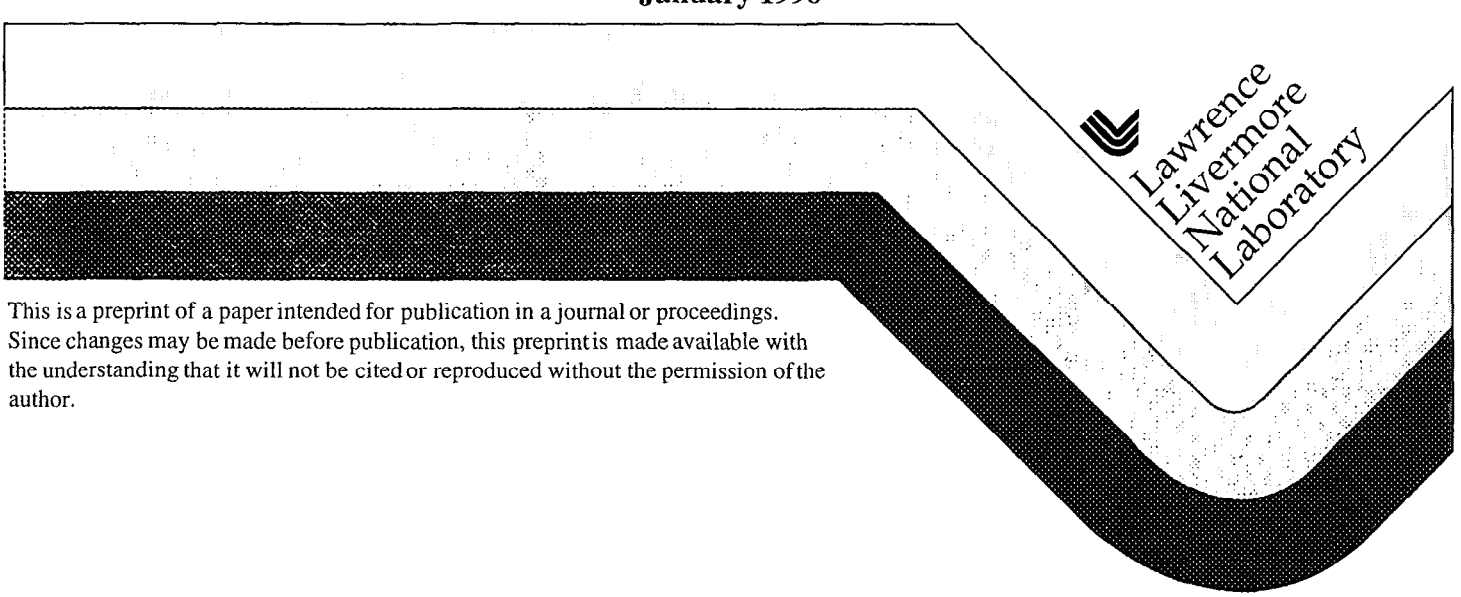

OCT for Diagnosis of Periodontal Disease

Bill W. Colston, Jr., Matthew J. Everett, Luiz B. DaSilva
Lawrence Livermore National Laboratory
Livermore, CA 94550

Linda L. Otis
University of Connecticut Health Center
Farmington, CT 06030

ABSTRACT

We have developed a hand-held *in vivo* scanning device for use in the oral cavity. We produced, using this scanning device, *in vivo* OCT images of dental tissues in human volunteers. All the OCT images were analyzed for the presence of clinically relevant anatomical structures. The gingival margin, periodontal sulcus, and dento-enamel junction were visible in all the images. The cemento-enamel junction was discernible in 64% of the images and the alveolar bone presumptively identified for 71% of the images. These images represent, to our knowledge, the first *in vivo* OCT images of human dental tissue.

Keywords: optical coherence tomography, OCT, dental, imaging, medical

1. BACKGROUND AND MOTIVATION

OCDR was first developed as a high resolution ranging technique for characterization of optical components[1]. The transverse scanning capability that made cross-sectional imaging (OCT) possible was subsequently applied to measurement of dielectric substrates in a coherence scanning microscope[2]. Both of these systems were based on bulk optics. The first fiber optic based OCDR system was constructed by the U. S. National Bureau of Standards for microoptic technology[3]. A group out of MIT headed by Dr. James Fujimoto then combined transverse scanning with a fiber optic OCDR system to produce the first OCT cross-sectional images of biological microstructure[4].

OCT was initially applied clinically to tomographic imaging of transparent tissue in the eye for diagnosis of retinal macular diseases[5]. Applying OCT to other clinically relevant biological structures, however, has been complicated by the problem of optical scattering[6]. The portion of backscattered photons from turbid tissue that passes the interferometric gate of the OCT system decays exponentially with depth. This rapid decay of signal from structural interfaces translates to shallow penetration depths (1-3 mm) in most biological tissue, making it impractical for many clinical applications. OCT has therefore been applied outside the retinal area to relatively accessible regions of the body, such as subsurface imaging of skin[7] or optical biopsy of the vascular system using catheter-based systems[8].

The oral cavity is another site on the body which has clinically relevant biological tissue in close proximity to the surface. Periodontal disease, in particular, involves morphological changes which are potentially detectable by an OCT system. A high-speed fiber-optic OCT system was developed in our lab for imaging and discrimination of hard and soft tissue structures in the oral cavity. *In vitro* OCT imaging studies were performed using porcine periodontal tissues[9, 10]. This successful implementation of the OCT dental system in animal models provided the impetus for construction of an improved *in vivo* imaging device. The images obtained with this system represent the first *in vivo* OCT images of human dental tissue.

2. MATERIALS AND METHODS

1. General OCT system design

A schematic of the OCT instrumentation is shown in Figure 1. It is based on a white light fiber optic Michelson interferometer. Output from a low coherence light source is split at the 2 x 2 fiber optic coupler and directed toward the sample and reference arms. Reflections from the mirror and backscattered light from the sample are recombined at the coupler and propagated to the detector and light source. Constructive interference creates a signal at the detector when the sample and reference reflections have traveled approximately the same optical group delay. The shorter the coherence length of the source, the more closely the sample and reference arm group delays must be matched for constructive interference to occur. By imposing a changing optical delay in the reference arm with a known velocity with a scanning mirror, the amplitudes and longitudinal positions of reflections from the sample can be measured with high accuracy.

A cross sectional image is produced by transversely scanning the beam across the sample and collecting a reflectance profile at each point. The reflectance intensities are recorded digitally on a gray-scale image as a function of transverse and axial distances. The OCT system was designed using a superluminescent diode centered at 1310nm, with a spectral bandwidth of 47 nm. The free space axial resolution of the system was 16 μm, with a sample arm power of 70 μW and a system dynamic range of 95dB. The total scan time for each image was approximately 45 seconds.

Figure 1 Schematic of OCT system design

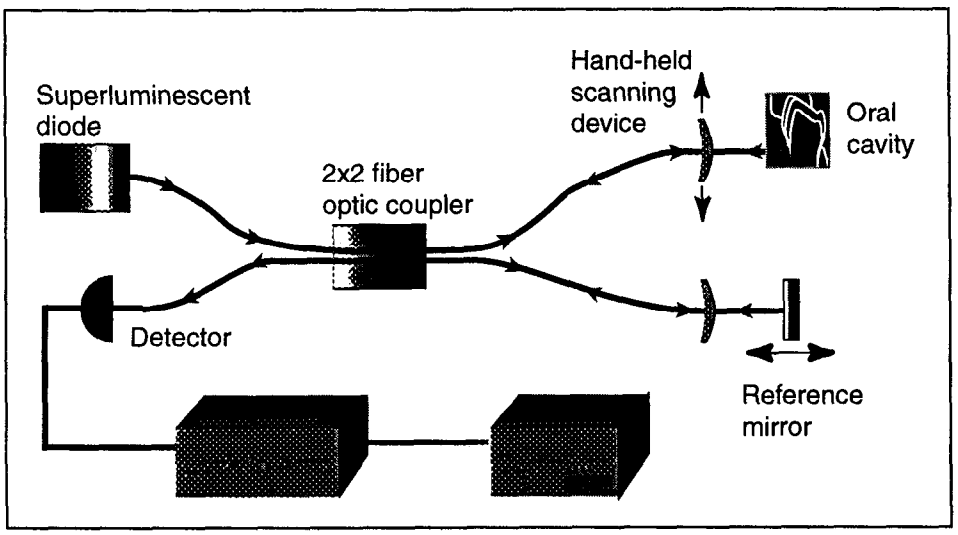

2. Hand held scanning device

A hand-held device was developed for *in vivo* measurements (Figure 2). The critical design requirements included comfortable access to the human oral cavity and a strategy for remotely scanning the sample arm collection optics to perform cross-sectional imaging. The collection optics were modified by using a gradient refractive index (GRIN) lens mounted on the end of the sample arm single mode fiber optic. Index matching ultraviolet curable epoxy was used at the fiber/GRINs interface to minimize refractive index mismatch. Transverse scanning of the fiber optic/GRIN lens assembly is accomplished through translation via a DC motor driven screw. Scan direction (up or down) is set through switches on the "trigger" portion of the probe. When either switch is depressed, a digital signal (generated from the DC motor power supply) is fed to the computer and used to apply an appropriate bias to the motor. Limit switches constrain lateral motion of the fiber assembly to the desired transverse scan dimension. A sterilizable removable tip is the only portion of the device in direct contact with the periodontal tissues. The distance from the end of the GRIN lens to the tissue contact point is adjusted by a screw-type mechanism at the interface with the probe main body.

The subfacial region of three volunteers was imaged using the hand-held scanner. The rear molars were excluded since access with the probe was limited. A total of 14 teeth from each volunteer was imaged in duplicate. Each image was subsequently analyzed to determine what portion of anatomical structures was visible.

Figure 2 Schematic of hand-held OCT scanner

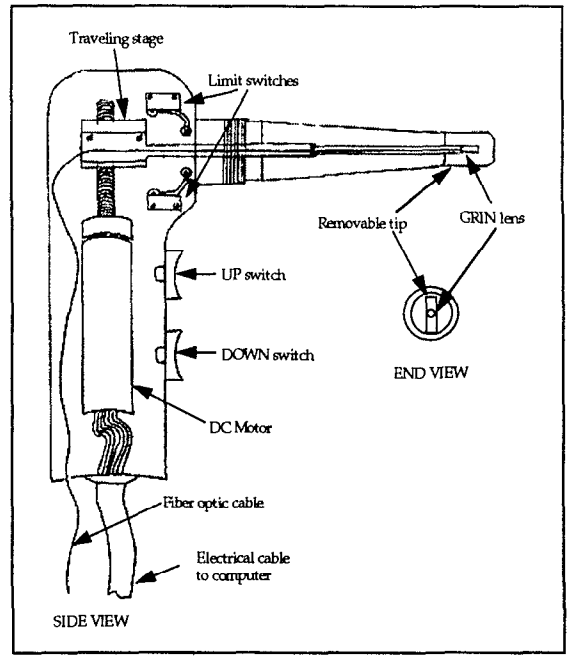

3. RESULTS AND DISCUSSION

1. *In vivo* imaging of dental structures

The results of the *in vivo* imaging studies revealed much more structural detail of the dental tissues than was visible from previous *in vitro* measurements. OCT images taken at the same anatomical location in the oral cavity from two volunteers are shown in Figure 3. A direct consequence of the system's enhanced signal to noise ratio is the improvement in penetration depth, increased one and a half times over prior instruments. Differences in pigmentation level between volunteers had limited effect on this depth. Variability in enamel morphology was also evident, with a sharp drop in the coherent backscattered intensity clearly delineating the junction between enamel and dentin layers. The enamel layer varied from 0.1 to 1 mm in thickness. Elevated signal levels marked the dento-epithelial junction, where the enamel surface of the tooth was visible behind the supra-alveolar connective tissue layer. The connective tissue (~0.3 mm), which is unkeratinized, is covered by a layer of fairly uniform keratinized junctional epithelium (~0.2 - 0.4 mm). Since keratin is a highly scattering component of soft tissue, the oral epithelium is more highly scattering and therefore darker in the grayscale intensity image than the underlying non-keratinized connective tissue. The junctional epithelium terminates at the mucogingival junction. The alveolar mucosa visible in the right hand image (~0.1 mm) continues below the image scan range to the mucous membrane of the cheek, lip, and floor of the oral cavity. The doppled region beneath the alveolar mucosa is porous alveolar bone (~0.3 mm). All the OCT images were analyzed for the presence of anatomical structures

which are clinically relevant. The gingival margin, periodontal sulcus, and dento-enamel junction were visible in all the images. The cemento-enamel junction was discernible in 64% of the images, and the alveolar bone presumptively identified for 71% of the images.

A coherent spike, visible as a vertical dark band of relatively constant intensity along the right side, was present in all the images. Measurements of the physical probe dimensions indicated this echo was due to a reflection from the front interface of the GRIN lens. Removal of this image artifact can be accomplished by changing the length of the GRIN lens and shifting the echo pathlength outside the focal range.

Figure 3 OCT images from identical periodontal region in two volunteers. Darker regions correspond to areas of larger backscattered intensity in units of dB. Scales are represented in terms of optical distance. Abbreviations: E-Enamel, D-Dentin, GM-Gingival Margin, DEJ-Dentoepithelial Junction, CT-Connective Tissue, JE-Junctional Epithelium, MGJ-Mucogingival Junction, AM-Alveolar Mucosa, AB-Alveolar Bone

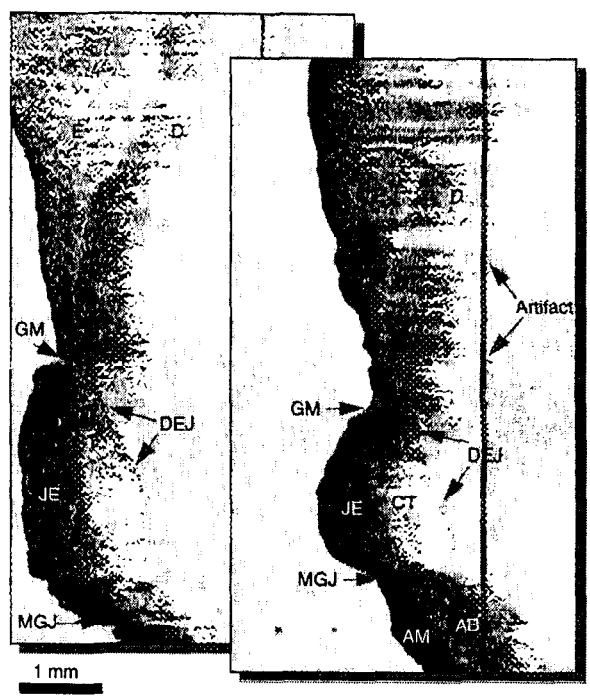

Motion artifacts were only present in 5% of the images (Fig 4). Motion artifacts that did occur were primarily low frequency modulations between adjacent longitudinal scans that were probably caused by patient breathing. Improvements in image acquisition time, feasible with a more powerful source or sacrifice of lateral resolution, would eliminate this problem. Faster acquisition times could also make direct contact with the tissue unnecessary, eliminating hygienic concerns associated with sterilization of the probe tip.

Figure 4 Consecutive OCT images from the same region of the periodontium in one volunteer. Right hand image demonstrates significant motion artifacts relative to left hand image. Abbreviations identical to
Figure 3.

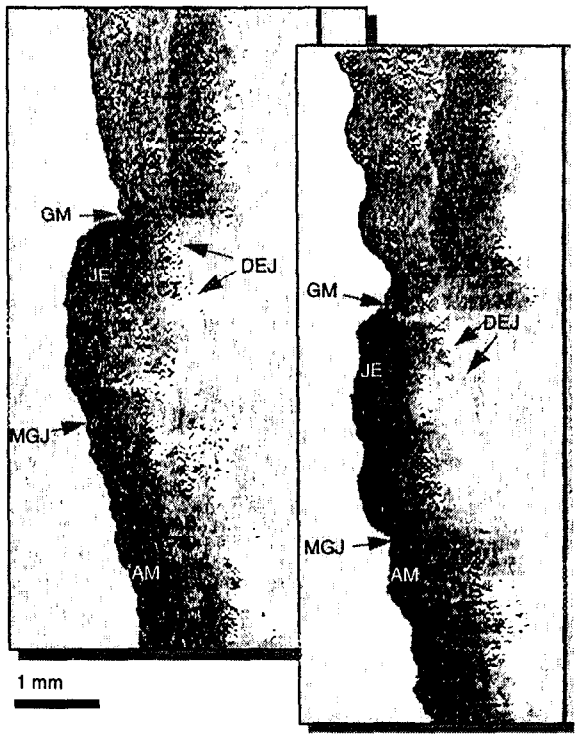

2. Dental restorations

Dental restorations are used to provide a barrier restricting oral fluids and bacteria from entering through the tooth into the systemic system as a result of dental decay or trauma. An inadequate seal can result in a further loss of tooth structure, infection, and dissemination of bacteria[11]. The most commonly used methods for evaluating the seal and structural integrity of restorations are visual and tactile examination[12,13]. OCT has the potential advantage over these methods of visualizing structural and marginal restoration defects before significant leakage occurs, minimizing tooth loss and decreasing the number of unnecessary replacement restorations.

A number of prosthetic materials, such as metals, composites, and ceramic fillings and caps, were imaged in this study. The tooth in Figure 5 left, for example, had a gold filling that extended to the outer surface. The presence of the highly reflective metal blocked penetration of the incident light and returned only a specular reflection at the air/tooth interface. The wavy contour of the tooth surface was created by motion artifacts. Since metal fillings and caps are integrated in the tooth structure, they complicate evaluation of hard tissue state but are unlikely to hinder diagnosis of gingival health. A second type of restoration material, porcelain, has much closer scattering properties to enamel, and therefore does not undermine image quality (Figure 5, right). The porcelain crown, which averaged over a millimeter in thickness, ended above the gingival margin. Directly below the crown is a band of highly reflective material (metal band) used to attach the prosthetic to the tooth. The junction between the porcelain crown and dentin microstructure is also clearly visible, raising the possibility of determining marginal integrity of the restoration/dentin interface with this technique

Figure 5 OCT images of periodontium with prosthetic materials implanted. Left - crown of tooth with gold cap. Right - Porcelain cap and associated gingival tissue. Abbreviations: GF - Gold Filling, P - Porcelain, others - as Figure 3.

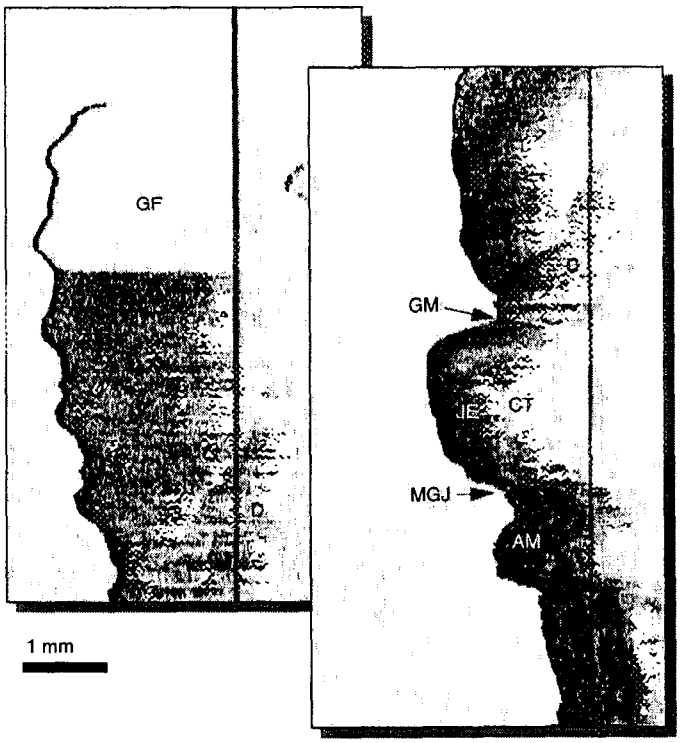

3. Imaging of dental hard tissues

Scans were also performed solely of hard tissue structures, parallel to the gingival margin (orthogonal to previous images), to determine the feasibility of OCT imaging for evaluating enamel microstructure. The interproximal region (between teeth), in particular, was imaged since caries incursion is most likely to occur in this area. Dental caries are a common disease that can be easily treated if detected early enough. If undetected and untreated, caries may progress through the outer enamel layer of a tooth into the softer dentin so far as to require extraction of the tooth or to cause inflammation of periodontal tissue surrounding the tooth. The standard methods for detecting caries in teeth are by visual inspection or by the use of dental x-rays. Both methods are unreliable for the detection of small caries. In addition, dental x-rays subject the patient to ionizing radiation, a known mutagen. OCT imaging offers the potential of a safe, noninvasive alternative for locating sites of caries incursion and therefore improves early disease detection and treatment.

The most remarkable finding in these data was the suggested presence of a double enamel layer (Figure 6). It is possible these two layers represent pre- and post-natal enamel formation. Enamel, composed almost entirely of hydroxyapatite, forms highly oriented prisms and is incapable of structural repair (remodeling). If, during enamel formation, the organism is under stress (disease, birth), the enamel deposited at that time may show irregularities in its calcification and subsequent disruption in the course of the enamel prisms. This results in formation of incremental lines (retzius) that mark the location of ameloblasts at the time of stress. This image therefore indicates post- and pre-natal enamel formation took approximately the same period of time, since the width of each layer is approximately 0.5 mm. The width of the line itself corresponds to the length of time the organism is stressed. The narrow extent of the incremental line in this figure supports the supposition that it occurred at birth. Cracks in the enamel layer, commonly prevalent near the more highly strained interproximal area, are also visible in this image. Although a more thorough study showing comparisons with histological sections is necessary to confirm

the nature of these structures, these images nevertheless represent the first *in vivo* visualization of enamel microstructure. Since caries represent regions of decalcified hard tissue, it is reasonable to expect OCT imaging systems would be capable of detecting them. Grooves or fissures in the occlusal surfaces of molars and premolars that can lead to a weakening of the tooth's defense against caries should also be visible. Accessibility of the probe tip to the area of interest is likely to be the limiting factors in this type of application.

Figure 6 OCT image of tooth and interproximal region.
Abbreviations: E1 - Enamel layer 1, E2- Enamel layer 2,
D- Dentin, IP - Interproximal region.

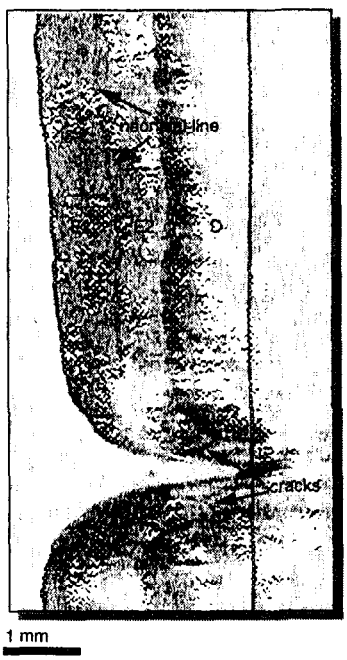

4. ACKNOWLEDGEMENTS

This work was performed under the auspices of the U.S. Department of Energy by Lawrence Livermore National Laboratory under Contract No. W-7405-Eng-48 and funded by a National Institute of Dental Research (NIDR) RO1 grant "Diagnostic Optimal Imaging of Periodontal Tissues."

5. REFERENCES

1. Youngquist, R. C., S. Carr, et al. "Optical coherence-domain reflectometry: a new optical evaluation technique." *Optics Letters* 12: 158-160,1987.

2. Lee, B. S. and T. C. Strand. "Profilometry With a Coherence Scanning Microscope." *Applied Optics* 29: 3784-3788,1990.

3. Danielson, B. L. and C. D. Whittenberg. "Guided-wave reflectometry with micrometer resolution." *Applied Optics* 26: 2836-2842,1987.

4. Huang, D., E. A. Swanson, et al. "Optical Coherence Tomography." *Science* 254: 1178-1181,1991.

5. Hee, M. R., C. A. Puliafito, et al. "Quantitative Assessment of Macular edema with optical coherence tomography." *Archives of Opthalmology* 113: 1019-1029,1995.

6. Yadlowsky, M. J., J. M. Schmitt, et al. "Multiple scattering in optical coherence microscopy." *Applied Optics* 34: 5699-5707,1995.

7. Schmitt, J. M., M. J. Yadlowsky, et al. "Subsurface imaging of living skin with optical coherence microscopy." *Dermatology* 191: 93-98,1995.

8. Tearney, G. J., S. A. Boppart, et al. "Scanning single-mode fiber optic catheter-endoscope for optical coherence tomography". *Optics Letters* 21: 543-545,1996.

9. Colston, B. W. Jr., M. Everett, et. al. "Imaging of hard and soft tissue structure in the oral cavity by optical coherence tomography." Submitted to Applied Optics, Sept. 1997.

10. Otis, L. L., B. W. Colston, G. Armitage, and M. J. Everett, "Optical Imaging of Periodontal Tissues." *Journal of Dental Research* 76(SI):383, 1997.

11. Leinfelder, K. F. and J. E. Lemons (1988). Clinical Restorative Materials and Techniques. Philadelphia, Lea & Febiger.

12. Cvar, J. F. and G. Ryge (1971). Criteria for the clinical evaluation of dental restoration materials. San Francisco, US Dept HEW PHS, Dental Health Center.

13. Dennison, J. B., J. M. Powers, et al. In vivo wear of posterior composite and amalgam restorations. *Journal of Dental Research* 59: 318,1980.

Technical Information Department • **Lawrence Livermore National Laboratory**
University of California • Livermore, California 94551